Cell, Vol. 123, 449–461, November 4, 2005, Copyright ©2005 by Elsevier Inc. DOI 10.1016/j.cell.2005.08.030

# Regulation of Cell Proliferation by a Morphogen Gradient

**Dragana Rogulja and Kenneth D. Irvine***
Howard Hughes Medical Institute, Waksman Institute, and Department of Molecular Biology and Biochemistry
Rutgers, The State University of New Jersey
Piscataway, New Jersey 08854

## Summary

**One model to explain the relationship between patterning and growth during development posits that growth is regulated by the slope of morphogen gradients. The Decapentaplegic (DPP) morphogen controls growth in the *Drosophila* wing, but the slope of the DPP activity gradient has not been shown to influence growth. By employing a method for spatial, temporal, and quantitative control over gene expression, we show that the juxtaposition of cells perceiving different levels of DPP signaling is essential for medial-wing-cell proliferation and can be sufficient to promote the proliferation of cells throughout the wing. Either activation or inhibition of the DPP pathway in clones at levels distinct from those in surrounding cells stimulates nonautonomous cell proliferation. Conversely, uniform activation of the DPP pathway inhibits cell proliferation in medial wing cells. Our observations provide a direct demonstration that the slope of a morphogen gradient regulates growth during development.**

## Introduction

The regulation of growth is a fundamental aspect of animal development—most organisms grow to reproducible sizes. Moreover, the growth of each organ is tightly regulated, such that appropriate proportions are achieved both between and within individual organs. It has long been hypothesized that reproducible regulation of size and proportion requires links between organ patterning and organ growth. The nature of these links, however, has remained unclear.

The developing *Drosophila* wing has served as a model for studies of organ growth and patterning. The wing forms from a cluster of undifferentiated cells in the larva, the wing imaginal disc. Over 4 days of larval development, the disc grows from approximately 40 cells to approximately 50,000 cells, which form a monolayered epithelial sac. Growth and patterning of the disc depend upon the determination of specialized cells along the borders between different compartments (reviewed in Irvine and Rauskolb, 2001; Lawrence and Struhl, 1996) (Figure 1A). Cells along the anterior-posterior (A-P) compartment border express a member of the BMP family of growth factors, Decapentaplegic (DPP) (Figure 1B), which spreads from its site of synthesis, forming a morphogen gradient (Entchev et al., 2000; Lecuit et al., 1996; Nellen et al., 1996; Teleman and Cohen, 2000). DPP signaling results in phosphorylation of a transcription factor, MAD, which can serve as a readout of the DPP activity gradient (reviewed in Padgett, 1999) (Figure 1C). Phospho-MAD and associated factors regulate the expression of downstream genes in a concentration-dependent manner to pattern the wing along the medial-lateral axis. Much of the regulation of downstream genes is effected through repression of a transcriptional repressor, Brinker (Campbell and Tomlinson, 1999; Jazwinska et al., 1999; Muller et al., 2003).

In addition to its role in wing patterning, DPP is a key regulator of wing growth. The growth of wings (and other imaginal discs) is severely impaired in *dpp* mutants, and clones of cells that cannot respond to *dpp* fail to proliferate and die (Burke and Basler, 1996; Lecuit et al., 1996; Spencer et al., 1982). Moreover, expression of DPP, or of an activated form of its receptor, Thickveins (TKV), can promote wing overgrowth (Burke and Basler, 1996; Capdevila and Guerrero, 1994; Lecuit et al., 1996; Nellen et al., 1996; Zecca et al., 1995). However, in the wild-type wing disc, growth is roughly even across the disc (Figure 1D) (Garcia-Bellido and Merriam, 1971; Milan et al., 1996; Resino et al., 2002), raising the fundamental question of how the gradient of DPP is translated into even growth.

A number of potential answers to this question have been considered. In threshold models, growth rate would be constant provided that levels of DPP exceed a minimum threshold. However, this could not explain how overexpression of DPP or of activated TKV promotes overgrowth. Inhibitor models postulate the existence of a growth inhibitor in a distribution that parallels the DPP activity gradient (Serrano and O'Farrell, 1997). However, no candidate inhibitors have been identified. It has also been suggested that patterning might be regulated by a basal gradient of DPP and growth by an apical, uniform distribution of DPP (Gibson et al., 2002). However, this would require two distinct intracellular transduction pathways for DPP signaling, for which there is no evidence. Finally, it has been hypothesized that growth might depend on the slope of the DPP gradient rather than its absolute levels (Gelbart, 1989; Lawrence and Struhl, 1996).

There is a long history of gradient models for growth regulation (Bohn, 1974; Day and Lawrence, 2000; French et al., 1976; Garcia-Bellido and Garcia-Bellido, 1998; Lawrence, 1970). Indeed, they precede the identification of actual morphogen gradients, as they were first conceived to explain regeneration (Bohn, 1974; French et al., 1976; Lawrence, 1970). When fragments corresponding to nonadjacent regions of an insect or amphibian limb are surgically juxtaposed, intercalary growth can occur to replace the intervening tissue. This led to models that linked growth to patterning, which posit that 1) cells in an organ assume distinct positional values, reflecting their location within a morphogen gradient (Wolpert, 1969); 2) cells compare their positional values with those of their neighbors; 3) significant discrepancies in positional values between neighbors stimulate

*Correspondence: irvine@waksman.rutgers.edu

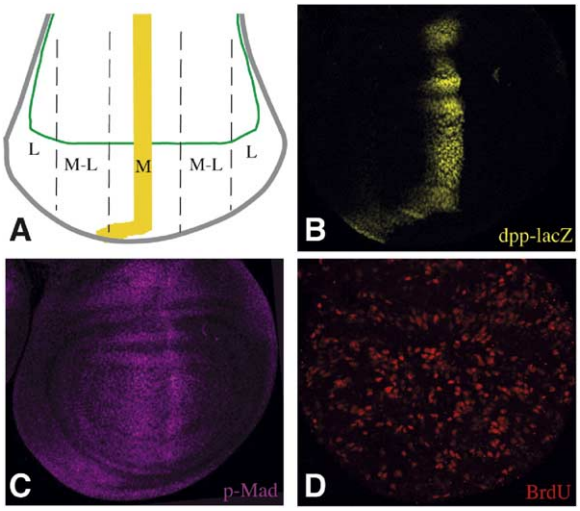


Figure 1. Organization of the Wing Imaginal Disc

(A) Schematic of the wing portion of a wing imaginal disc, with the approximate location of DPP-expressing cells (yellow) and dorsal-ventral boundary cells (green) indicated. The subdivision of the wing into lateral (L), medial-lateral (M-L), and medial (M) regions used for scoring clones is also indicated.

(B) Location of DPP-expressing cells, visualized by staining a *dpp-lacZ* line.

(C) TKV activity gradient in the wing, visualized by staining for phospho-MAD.

(D) Distribution of cell proliferation in the wing, visualized by labeling and staining for BrdU.

cell proliferation; and 4) daughter cells acquire positional values intermediate between their neighbors, such that the discrepancies in positional values become more shallow until proliferation ceases.

Although the observations that DPP forms a morphogen gradient and is required for growth are consistent with the possibility that growth is actually stimulated by a gradient of positional values specified downstream of DPP, several observations have appeared to contradict this hypothesis. First, the DPP gradient and its associated activity gradient decay exponentially rather than linearly (Entchev et al., 2000; Teleman and Cohen, 2000); thus, it is not clear how mechanisms tied to the slope of the gradient could generate even growth across the disc. Second, uniform expression of DPP, or of activated TKV, can promote wing overgrowth (Lecuit et al., 1996; Martin-Castellanos and Edgar, 2002; Nellen et al., 1996), implying that growth is affected by the level of DPP and is not limited to situations where DPP is graded. Moreover, expression of activated TKV in clones has been reported to promote proliferation in a strictly cell-autonomous manner, whereas gradient models would predict that it should promote proliferation nonautonomously. Thus, despite the theoretical appeal of gradient models and their ability to explain regeneration, experiments with a key morphogen that actually patterns the wing and regulates its growth have appeared to contradict them.

In order to re-examine the relationship between DPP pathway activity and wing growth, we created a method for controlled gene expression that allows quantitative and temporal control over gene expression in clones of cells. Using this approach, we demonstrate that the juxtaposition of cells perceiving different levels of DPP signaling does in fact stimulate nonautonomous proliferation. We further show that the responses to DPP differ in lateral versus medial regions of the disc and that the nonautonomous proliferative response is transient, suggesting explanations for why the nature of growth regulation by DPP was missed in prior experiments. By establishing the fundamental ability of the DPP gradient to regulate growth, our results provide a molecular basis for linking growth to patterning in developing tissues.

## Results

### A Method for Conditional Gene Expression in Genetic Mosaics

Studies of the influence of the DPP pathway on wing growth and patterning have, for technical reasons, focused on long-term responses, typically involving at least 2 days between pathway modulation and response assessment. However, we reasoned that cells might adapt to changes in DPP signaling, in which case short- and long-term responses could differ. To evaluate this possibility, we developed a system for temporal regulation of gene expression in genetic mosaics.

This was achieved by combining the UAS-Gal4 (Brand and Perrimon, 1993), Flp-out (Struhl and Basler, 1993), and GeneSwitch Gal4 (Osterwalder et al., 2001; Roman et al., 2001) methods for regulating gene expression. A *Gal4:Progesterone Receptor* fusion gene (*Gal4:PR*) (Osterwalder et al., 2001) was inserted into an *actin* promoter Flp-out cassette (Struhl and Basler, 1993) to generate a transgene we refer to as *AyGal4:PR* (Figure 2A). Based on prior studies of the component parts, we expected that, in transgenic flies, a pulse of expression of the Flipase enzyme would catalyze excision of a DNA cassette containing a transcriptional terminator, allowing expression of Gal4:PR in clones of cells. In the absence of hormone, the PR domain would prevent Gal4 from activating transcription, but, in the presence of a progesterone analog, RU486, this repression would be relieved, resulting in expression of transgenes under the control of UAS regulatory sequences (Figure 2). An additional advantage of this system is that changes in RU486 concentration can lead to quantitative changes in target gene expression (Osterwalder et al., 2001).

Experimental analysis confirmed that the AyGal4:PR system works as expected (Figure 2). RU486 was delivered by transferring larvae to RU486-containing food. GFP expression is barely detectable in association with *AyGal4:PR* clones in larvae containing a *UAS-GFP* transgene but grown on normal food (Figure 2D). GFP-expressing clones can, however, be readily visualized within 4 to 5 hr after their transfer to RU486-containing food (Figure 2E). Expression levels increase strongly up to 10–15 hr after drug addition (Figure 2F), after which they appear to plateau (data not shown).

### Controlled Activation of TKV in Clones

In order to analyze the temporal response to mosaic activation of the DPP pathway, Gal4:PR-expressing clones

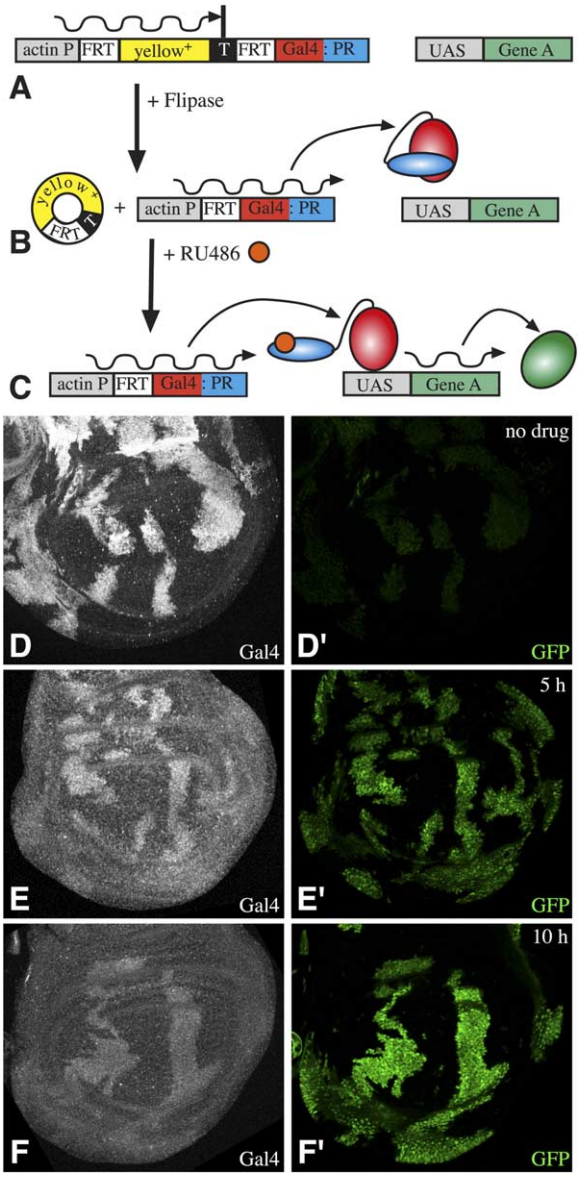


Figure 2. Regulation of Gene Expression by AyGal4:PR

(A) The *AyGal4:PR* transgene includes an *actin* promoter, two Flip recombination target (FRT) sites flanking a wild-type copy of *yellow* and a transcriptional terminator (T), followed by the Gal4 coding region fused to the Progesterone Receptor ligand binding domain (Gal4:PR). In flies containing *AyGal4:PR*, transcription terminates before Gal4:PR.

(B) Expression of Flipase can catalyze recombination between the FRT sites, resulting in excision of the *yellow+* terminator cassette, to generate an *actin>Gal4:PR* transgene. Without the addition of RU486, however, the Gal4:PR protein is unable to activate transcription.

(C) Upon addition of RU486, the repression of transcription effected by the PR ligand binding domain is relieved, allowing expression of UAS transgenes.

(D–F) Wing imaginal discs from *AyGal4:PR UAS-GFP* animals at 0 (D), 5 (E), and 10 (F) hr after transfer to media containing 20 μg/ml RU486. Expression of Gal4:PR was visualized by anti-Gal4 DNA binding domain sera (white), and expression of GFP appears green. These discs are taken from animals cultured and stained in parallel, so the elevation in GFP fluorescence from (D) to (F) is reflective of its increased expression. Gal4 staining declines upon drug addition, suggesting that the epitopes recognized by the sera become less accessible.

were generated in flies carrying an activated form of TKV under UAS control. We examined responses to two different transgenes, one with an extracellular ligand binding domain ($TKV^{Q253D}$) (Nellen et al., 1996) and one without it ($TKV^{DEQ199D}$) (Haerry et al., 1998). Both forms are constitutively active as a consequence of phosphorylation-mimicking substitutions in the intracellular domain, and we refer to them generically as $TKV^{Q-D}$. Because expression of $TKV^{Q-D}$ can induce some apoptosis in wings (Adachi-Yamada et al., 1999; Adachi-Yamada and O'Connor, 2002), in many experiments, we also coexpressed the pancaspase inhibitor p35.

Gal4:PR-expressing clones were induced during the first larval instar (24–48 hr after egg laying) and allowed to grow for 10–55 hr in the absence of RU486. Larvae were then transferred to RU486-containing food, initiating the expression of $TKV^{Q-D}$. Wing discs from these larvae were analyzed at 2–3 hr intervals, over a period of 5–50 hr on RU486, with the endpoint of all experiments set at 96 ± 12 hr after egg laying, which corresponds to the middle of the third larval instar. The responses observed were similar throughout this age range. To assay the influence of $TKV^{Q-D}$ on proliferation, discs were labeled with BrdU, a thymidine homolog that is incorporated into replicating DNA and can be detected by immunostaining. BrdU labeling is elevated by a variety of manipulations that stimulate growth in *Drosophila*, including activation of TKV (Martin-Castellanos and Edgar, 2002). In wild-type discs, or in control discs expressing GFP or p35 in clones, a 30 min pulse of BrdU labeling results in staining that is locally inhomogeneous but distributed essentially evenly throughout the disc (Figures 1 and 3J and data not shown) (Milan et al., 1996). In the absence of RU486, *AyGal4:PR UAS-tkv$^{Q-D}$* clones did not exhibit detectable effects on either phospho-MAD staining or BrdU incorporation (data not shown). Importantly then, clones of cells expressing $TKV^{Q-D}$ were associated with both an autonomous elevation of BrdU labeling in lateral cells (Martin-Castellanos and Edgar, 2002) and a strong nonautonomous elevation of BrdU labeling (Figure 3).

## Autonomous Induction of Cell Proliferation by $TKV^{Q-D}$

A strong elevation of BrdU labeling in response to $TKV^{Q-D}$ occurs within clones in lateral regions of the disc, where the endogenous levels of DPP signaling are lowest. In these clones, BrdU staining is elevated both in terms of the number of cells staining and in their intensity of labeling, which indicates both that more cells are in S phase and that they are replicating more rapidly (Figure 3). The increase in BrdU labeling occurs quickly, as in some cases it could be detected within 5 hr after transfer of larvae to RU486-containing food (17 of 51 lateral clones at 5 hr; Figure 3A). Elevated BrdU labeling in lateral clones was detectable throughout the time course of the experiment, consistent with studies that have examined long-term responses to DPP pathway activation (Figure 3; Table 1) (Lecuit et al., 1996; Martin-Castellanos and Edgar, 2002; Nellen et al., 1996).

In medial regions of the disc, autonomous stimulation of BrdU labeling was relatively weak and uneven (Figure

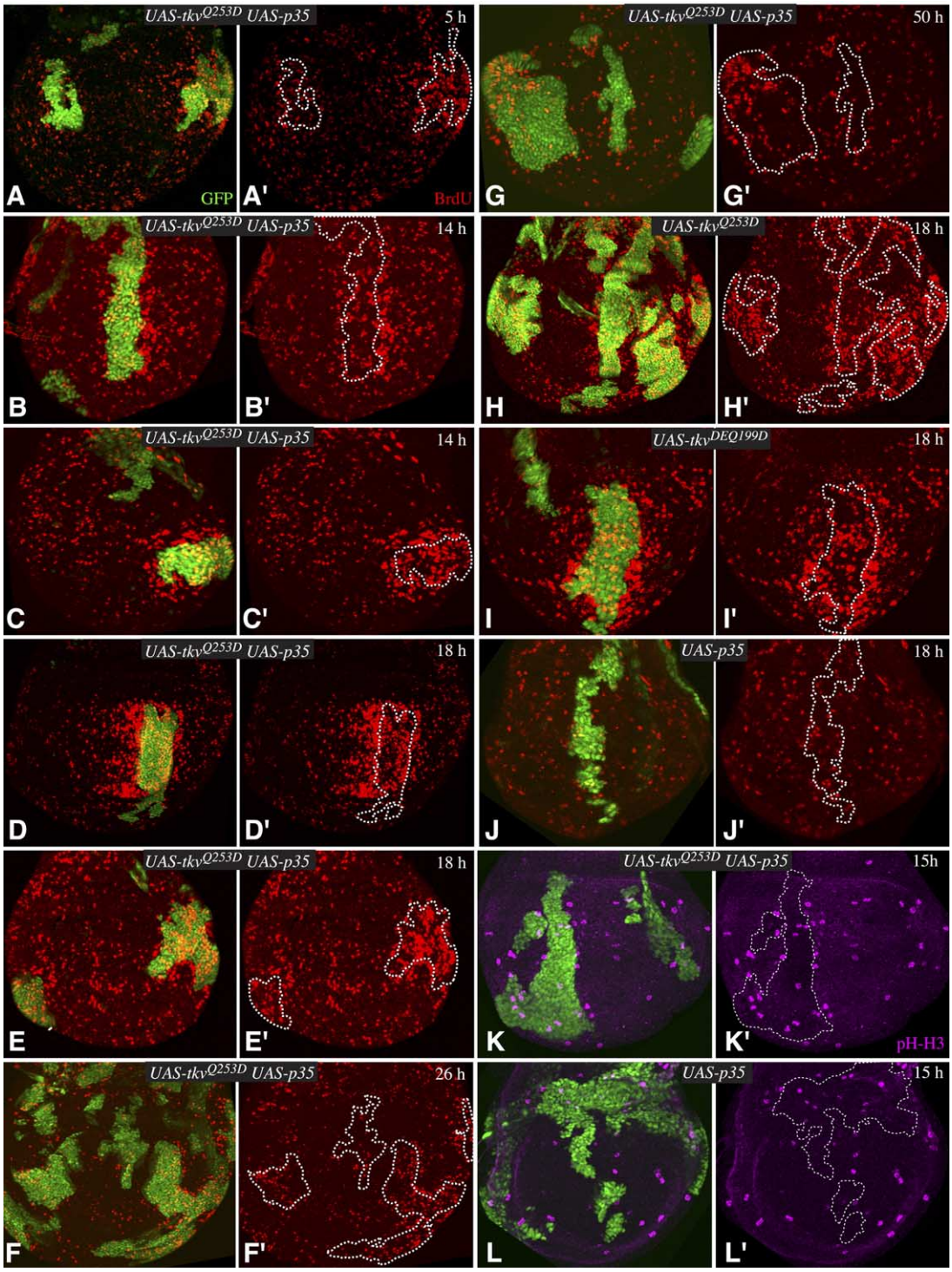


Figure 3. Clonal Induction of TKV$^{Q-D}$ Expression Induces Autonomous and Nonautonomous Cell Proliferation

All panels show wing imaginal discs containing Gal4:PR-expressing clones marked by expression of GFP (green) and grown for the indicated number of hours on media containing 20 μg/ml RU486 and labeled and stained for BrdU (red) or pH-H3 (magenta). Panels marked (′) show single channels of the stain to the left. For ease of comparison, the locations of selected clones are outlined by dashes. Because the nuclei are not all in the same focal plane, in this and other figures, we combined staining in different focal planes by maximum projection through confocal sections. In cases where the cells are not vertical, this can create an artifactual "spread" of the clone edges, in which case clone borders were drawn with reference to single optical sections.

(A–G and K) Clones in animals with *AyGal4:PR UAS-tkv*$^{Q253D}$ *UAS-p35 UAS-GFP* transgenes at the indicated times after transfer to RU486 media. In terms of the range of nonautonomous responses to TKV$^{Q-D}$, the clone in (D) exemplifies the most extreme effects observed, the right clone in (E) exemplifies a mild effect, and the left clone in (E) is without evident effect.

(H–J and L) Clones in animals with *AyGal4:PR* and *UAS-tkv*$^{Q253D}$ *UAS-GFP* (H), *UAS-tkv*$^{DEQ199D}$ *UAS-GFP* (I), or *UAS-p35 UAS-GFP* (J and L) transgenes, grown for 18 or 15 hr after transfer to RU486 media.

Table 1. Influence of AyGal4:PR Clones on BrdU Labeling

| | Autonomous Effect | | | | Nonautonomous Effect | | | |
|---|---|---|---|---|---|---|---|---|
| | Enhance | Repress | None | Complex/ Unsure | Enhance | Repress | None | Complex/ Unsure |
| $TKV^{Q253D}$ + p35 Clones at 12–14 hr Postinduction | | | | | | | | |
| Lateral (n = 34) | 24 | | 8 | 2 | 13 | | 11 | 10 |
| Medial-lateral[a] (n = 98) | 43 | 2 | 37 | 16 | 62 | | 30 | 6 |
| Medial (n = 36) | 6 | 1 | 19 | 10 | 24 | | 10 | 2 |
| p35 Clones at 12–14 hr Postinduction | | | | | | | | |
| Lateral (n = 16) | | | 16 | | | | 16 | |
| Medial-lateral (n = 46) | 2 | | 44 | | 2 | | 44 | |
| Medial (n = 17) | | | 17 | | | | 17 | |
| $TKV^{Q253D}$ + p35 Clones at 50 hr Postinduction | | | | | | | | |
| Lateral (n = 33) | 14 | | 17 | 2 | 4 | 1 | 26 | 2 |
| Medial-lateral (n = 49) | 5 | 3 | 27 | 14 | 8 | 1 | 36 | 4 |
| Medial (n = 30) | | 5 | 23 | 2 | 2 | | 24 | 4 |
| p35 Clones at 50 hr Postinduction | | | | | | | | |
| Lateral (n = 21) | 1 | 1 | 19 | | 1 | | 20 | |
| Medial-lateral (n = 20) | | 1 | 19 | | | | 20 | |
| Medial (n = 13) | | | 13 | | | | 13 | |

A set of micrographs including $TKV^{Q253D}$- and p35-expressing clones, induced with 20 μg/ml RU486 for the indicated number of hours, were scored blind for effects on BrdU staining. Clones in different regions of the disc (Figure 1) were scored separately (n = number scored), and each clone was scored for both effects on proliferation within the clone (autonomous effect) and effects on proliferation of neighboring cells (nonautonomous effect). Effects were judged in comparison to regions of the same disc without clones. The complex/unsure class includes clones that had substantially different effects in different regions (e.g., activation in one area but repression in another) or cases in which a confident assignment could not be made because the effect was weak.

[a] This class includes both clones that lie entirely within this region and clones that span adjacent regions.

3; Table 1; Table S1). Indeed, some clones appear as a "shadow" of cells that proliferate less than their wild-type neighbors (Figures 3B and 3I). The relatively weaker labeling of medial clones (Figure 3B; cf. Figure 3C) is consistent with observations that $TKV^{Q-D}$-expressing clones proliferate less medially than they do laterally (Lecuit et al., 1996; Martin-Castellanos and Edgar, 2002; Nellen et al., 1996). In medial-lateral regions (see Figure 1), clones exhibited intermediate phenotypes in terms of the autonomous elevation of BrdU labeling, generally correlating with the relative location of the cells in the clone along the medial-lateral axis (Figures 3D–3G).

### Nonautonomous Induction of Cell Proliferation by Activated TKV

The most striking aspect of the $TKV^{Q-D}$-clonal behavior is the nonautonomous stimulation of BrdU labeling, which has not been described previously. As for the autonomous response, BrdU staining is elevated both in terms of the number of cells staining and the intensity of labeling. This nonautonomous stimulation can occur adjacent to both medial and lateral clones. The effect is most intense in cells immediately adjacent to $TKV^{Q-D}$ clones but is often discernible a few cell diameters away (Figure 3). Nonautonomous stimulation is occasionally detectable as early as 5 hr after pathway activation, but the initial effect is weak (Figure 3A). It becomes stronger by 8–10 hr, appears to peak around 12–14 hr, and remains strong until 18–24 hr after induction (Figures 3B–3E, 3H, and 3I). After 24 hr, cells surrounding most medial clones no longer exhibit substantially elevated BrdU labeling (Figure 3F). The nonautonomous effect appears to persist longer in lateral regions but eventually declines there as well, such that, by 50 hr, only the autonomous response to TKV activation is consistently observed (Figure 3G; Table 1).

There is some variability in BrdU staining in wild-type wing discs. In addition, there is variability in the detection of BrdU labeling associated with $TKV^{Q-D}$-expressing clones. To ensure objective evaluation, a number of clones at 12–15 hr and 50 hr time points were scored blindly for effects on BrdU labeling. In this analysis, 66% of the $TKV^{Q-D}$-expressing clones were scored as causing some nonautonomous elevation in BrdU staining at 12–15 hr (as compared to regions of the disc that lacked clones), while only 6% of control clones were scored as having a nonautonomous effect (Table 1 and Table S1). Although the reasons for the incomplete penetrance of this effect (or our ability to detect it) are not yet clear, the observation that BrdU labeling is stimulated in wild-type cells when they neighbor cells in which the DPP pathway is activated to high levels suggests that proliferation can be stimulated in the developing wing by the juxtaposition of cells that have acquired different positional values through the action of the DPP pathway, as predicted by gradient models of growth control.

While elevated BrdU incorporation normally correlates with cell proliferation, it is formally only a marker of DNA replication. To determine whether nonautonomous elevation of DNA replication is accompanied by progression through the cell cycle, cells were stained for anti-phosphohistone H3 (pH-H3), which labels cells in M phase. Because wing-disc cells spend only a short time in M phase, relatively few cells are labeled by anti-pH-H3. Nonetheless, an increase in pH-H3 staining rel-

ative to other regions of the disc was observed among cells neighboring TKV$^{Q-D}$-expressing clones (Figures 3K and 3L; in blind scoring, 40 of 74 TKV$^{Q-D}$-expressing clones at 15 hr, but only 1 of 50 control clones, were associated with a nonautonomous increase in pH-H3 stained cells). As a third marker of cell proliferation, we examined a PCNA-GFP fusion that is regulated by E2F and reports patterns of cell proliferation in multiple *Drosophila* tissues (Thacker et al., 2003). PCNA-GFP expression in the wing is heterogeneous but often appeared to be higher than average among cells near TKV$^{Q-D}$-expressing clones (Figure S1; in blind scoring, 29 of 48 TKV$^{Q-D}$-expressing clones at 15 hr, but only 6 of 44 control clones, were associated with a local increase in PCNA-GFP expression). Staining for total DNA content, and for cell size using basolateral- and apical-membrane markers, revealed that cells surrounding TKV$^{Q-D}$ clones exhibit normal DNA staining and size distributions (Figure S1 and data not shown). This indicates that the accelerated cell-cycle progression revealed by staining with molecular markers is coupled to normal cellular growth and is reflective of elevated cell proliferation.

### Activated-TKV Does Not Exert Nonautonomous Influences on the DPP Pathway

Even though prior studies have only reported autonomous effects of activated-TKV on the DPP pathway, a nonautonomous effect on DPP signaling might be considered as a trivial explanation for the nonautonomous stimulation of proliferation. For example, expression of TKV$^{Q-D}$ distorts the endogenous DPP gradient because receptor levels influence gradient formation and the transcription of endogenous *tkv* is downregulated by DPP signaling (Lecuit and Cohen, 1998). However, both TKV$^{Q253D}$, which includes the extracellular, ligand binding domain, and TKV$^{DEQ199D}$, which does not, exert similar effects on cell proliferation (Figure 3; Table 1; Table S1; data not shown), whereas their effects on the endogenous DPP gradient are expected to be opposite. In a more direct test, we examined phosphorylation of the MAD transcription factor. Elevation of phospho-MAD staining associated with TKV$^{Q-D}$-expressing cells is strictly cell autonomous (Figures 4A and 4B). Thus, the nonautonomous effects of TKV$^{Q-D}$ on cell proliferation do not result from influences on DPP signaling in neighboring cells.

### Nonautonomous Proliferation Is Not a Secondary Consequence of Cell Death or Growth

Activation of apoptosis can stimulate the proliferation of neighboring cells, a process referred to as compensatory proliferation (Huh et al., 2004; Perez-Garijo et al., 2004; Ryoo et al., 2004), and expression of TKV$^{Q-D}$ can induce apoptosis (Adachi-Yamada et al., 1999; Adachi-Yamada and O'Connor, 2002). However, while keeping cells "undead" through p35 expression has been reported to potentiate compensatory proliferation (Huh et al., 2004; Perez-Garijo et al., 2004; Ryoo et al., 2004), the presence or absence of p35 did not noticeably influence the nonautonomous effects of TKV$^{Q-D}$ (Figures 3B-3E; cf. Figures 3H and 3I; Table 1; Table S1). Nonetheless, to directly address the possibility that activation of apoptosis contributes to the nonautonomous effects of TKV$^{Q-D}$, we stained with an antibody against an activated form of the Drice caspase. Some apoptosis is detected in our experiments, but not until 35 hr after the induction of TKV$^{Q-D}$ expression, which is well after the initiation of cell proliferation, and even then only a fraction of clones (10 of 50) exhibited detectable levels of apoptosis (Figure S2). Additionally, compensatory proliferation is associated with induction of Wingless (WG) and DPP expression, but *dpp-lacZ* is not induced by TKV$^{Q-D}$ clones, and WG is only induced in cells in a

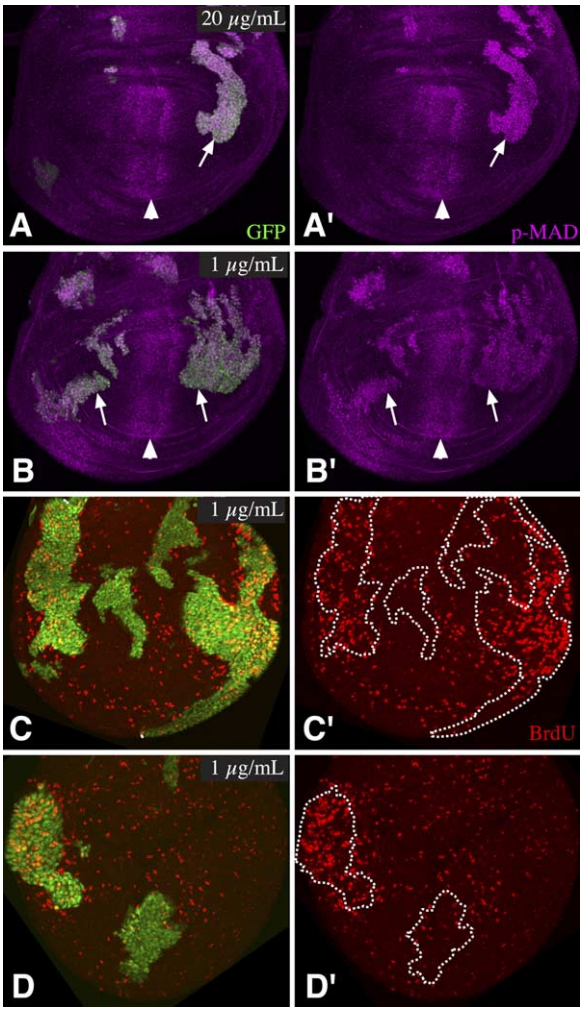


Figure 4. Responses to AyGal4:PR Are Dependent upon the Dose of RU486

All panels show discs containing Gal4:PR-expressing clones from *AyGal4:PR UAS-tkv$^{Q253D}$ UAS-p35 UAS-GFP* animals, marked by expression of GFP (green) and grown for 18 hr on media containing RU486. In (A) and (B), discs were stained with antibodies against phospho-MAD (magenta).

(A) At 20 μg/ml, p-MAD is induced (arrows) at levels above peak endogenous levels (arrowhead).

(B) At 1 μg/ml, p-MAD is induced (arrows) at levels comparable to peak endogenous levels (arrowhead).

(C and D) Discs induced with 1 μg/ml RU486 and then labeled and stained for BrdU (red). Lateral clones have mild nonautonomous effects, while medial clones have no evident effect.

narrow region near the D-V boundary, which cannot account for the proliferative effects observed (Figure S2).

We also considered the possibility that nonautonomous proliferation might be a generic response to excessive proliferation within a local region. This seemed unlikely because TKV$^{Q-D}$ clones do not stimulate much autonomous proliferation in medial regions but do stimulate medial nonautonomous proliferation. Nonetheless, as a more direct test, we coexpressed the growth-promoting proteins cyclin D and Cdk4 in *AyGal4:PR* clones. These clones ultimately overgrow, as in conventional Flp-out clones (Datar et al., 2000), but no nonautonomous stimulation of cell proliferation was detected (Figure S2).

The results described above provide support for the hypothesis that nonautonomous proliferation is induced by juxtaposition of cells with different positional values by ruling out alternative explanations. Below, we describe three direct tests of this hypothesis.

### Uniform Activation of TKV Induces Lateral Proliferation but Inhibits Medial Proliferation

First, we examined the temporal response to uniform TKV activation. This would be expected to stimulate cell-autonomous responses to TKV but to inhibit responses that require the juxtaposition of cells with different positional values. Temporally controlled uniform pathway activation was achieved using a derivative of the *AyGal4:PR* transgene insertion, *actin>Gal4:PR*, from which the transcriptional terminator cassette had been permanently excised by Flp-out in germline cells (Figure 1B). Animals containing this transgene were crossed to animals with *UAS-GFP* (control) or *UAS-GFP* and *UAS-tkv$^{Q-D}$* (experimental) transgenes. In the absence of drug, there were no detectable effects on BrdU labeling in wing discs (Figure 5A). Animals were raised in the absence of RU486 and then transferred to RU486-containing food and analyzed as described above after 6, 12, 18, or 24 hr. Phospho-MAD staining confirmed that strong uniform activation of the pathway occurred within 18 hr (Figure 5F). At 6 hr, only subtle effects on BrdU labeling could be detected (Figure 5B), but, by 12 hr, elevated staining in lateral cells, but not in medial cells, was consistently observed (Figure 5C). By 18 hr, this effect is even more pronounced: many lateral cells have high levels of BrdU staining, medial-lateral cells have moderate levels of BrdU staining, and medial cells are virtually devoid of BrdU staining (Figure 5D; cf. Figure 5A). The induction of proliferation is not uniform throughout lateral cells, however, as in general it appears greatest in cells closer to the D-V boundary (Figure 5D; cf. Figure 1A), which might explain some of the variability observed in mosaic-expression experiments (Figure 3; Table 1; Table S1). Uniform expression of TKV$^{Q-D}$ also results in elevation of pH-H3 staining in lateral regions and inhibition of pH-H3 staining in medial regions (data not shown).

Thus, as in the autonomous response to clonal activation, upon uniform activation, lateral, but not medial, cells exhibit a strong proliferative response to TKV. Moreover, the absence of detectable proliferation in medial regions upon uniform activation (Figure 5D) provides a critical contrast to the medial proliferation induced both inside and outside of TKV$^{Q-D}$ clones (Figure 3), as these experiments include insertion of the same promoter at the same chromosomal location and iden-

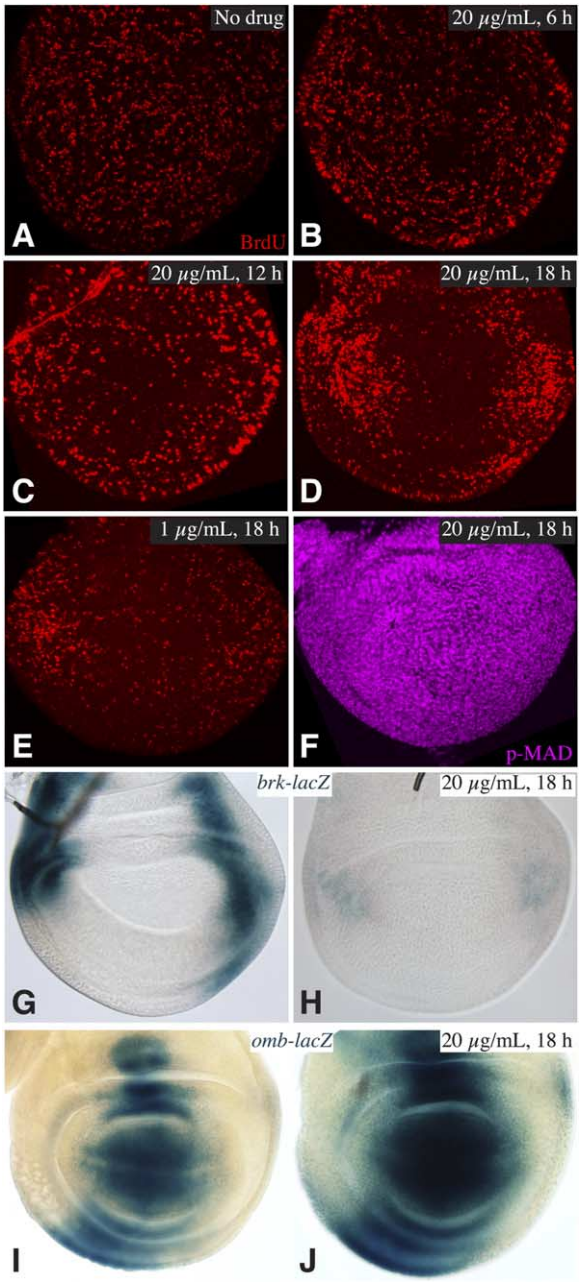


Figure 5. Uniform Expression of TKV$^{Q-D}$

(A)–(F), (H), and (J) show discs from *actin>Gal4:PR UAS-tkv$^{Q253D}$ UAS-GFP* animals. (A) was grown on media without RU486. (B)–(F) were grown for the number of hours indicated on media containing RU486 and then labeled and stained for BrdU (red, [A–E]) or phospho-MAD (magenta, [F]). (B)–(D) and (F) were grown on 20 μg/ml RU486; (E) was grown on 1 μg/ml RU486. The slight variation in intensity in (F) is reflective of focal plane and nuclear density. (G)–(J) show discs from animals carrying a *brk-lacZ* reporter line ([G and H], stained in parallel) or an *omb-lacZ* reporter line ([I and J], stained in parallel). (G) and (I) show wild-type controls; (H) and (J) show discs 18 hr after induction of uniform TKV$^{Q-D}$ expression.

tical time points and drug doses. Thus, medial-cell proliferation requires the juxtaposition of cells with different levels of TKV activity.

To examine the influence on known downstream targets, discs were stained for expression of a gene repressed by DPP signaling, *brinker (brk)*, and two genes activated downstream of DPP signaling, *optomotor blind* (*omb*) and *spalt*. *brk* expression was substantially repressed within 18 hr (Figure 5H). The lateral proliferation induced by $TKV^{Q-D}$ is likely effected through the decrease in *brinker* levels, as loss of *brinker* results in an autonomous elevation of proliferation in lateral cells (Campbell and Tomlinson, 1999; Jazwinska et al., 1999; Martin et al., 2004). Interestingly, however, *omb* (Figure 5J) and *spalt* (data not shown) were only weakly induced within lateral cells at 18 hr, even though $TKV^{Q-D}$ has dramatic affects on proliferation by this time (Figure 5D). Thus, *omb* and *spalt* are unlikely to participate in the proliferation induced by $TKV^{Q-D}$.

### Nonautonomous Proliferation Depends on Quantitative Differences in TKV Activation

Another prediction of gradient models for growth regulation is that the induction of cell proliferation should depend on the difference in levels of pathway activation between neighboring cells. In the experiments described above (Figure 3), a high drug dose (20 μg/ml) was used, resulting in levels of pathway activation above the normal peak levels of activation in the middle of the disc (Figure 4A). By feeding larvae different concentrations of RU486, however, the level of pathway activation in clones can be varied. Under lower-drug-dose conditions (1 μg/ml), the level of pathway activation, as monitored by phospho-MAD staining, is comparable to the normal levels of activation in the medial part of the disc (Figure 4B). While in lateral and medial-lateral regions both nonautonomous and autonomous induction of proliferation is still induced by this lower level of $TKV^{Q-D}$ expression, the effect is weaker, and in medial regions induction of proliferation is almost never observed (Figures 4C and 4D). Thus, nonautonomous stimulation of proliferation is dependent upon the difference in the levels of TKV activation between neighboring cells. Additionally, the ability to stimulate proliferation noticeably above wild-type rates apparently requires differences in juxtaposed cell fates that are greater than those that already exist within the endogenous TKV activity gradient.

We also examined the consequences of lower-level activation under uniform expression conditions (*actin>Gal4:PR*). This was associated with milder effects than high-level uniform activation, in terms of both the stimulation of BrdU labeling in lateral regions and the inhibition of BrdU labeling in medial regions (Figure 5E; cf. Figure 5D). As this low-level uniform expression is expected not to eliminate the TKV activity gradient but to decrease its slope, the moderate inhibition of BrdU labeling in the medial wing further supports the inference that the rate of proliferation here is proportional to the steepness of the TKV activity gradient.

### Nonautonomous Induction of Cell Proliferation by Inhibition of DPP Signaling

If proliferation is stimulated simply by the juxtaposition of cells that perceive different levels of DPP signaling, rather than by the activation of the pathway per se, it should be possible to stimulate proliferation not only by making clones of cells in which the pathway is autonomously activated but also by making clones of cells in which the pathway is autonomously inhibited. To examine this, we made clones of cells that expressed either *daughters against dpp* (*dad*) or *brk*. *dad* encodes an inhibitor of the DPP pathway that is induced by DPP signaling and acts by competitively interfering with MAD (Tsuneizumi et al., 1997). *brk* encodes a transcriptional repressor that is repressed by DPP signaling (Campbell and Tomlinson, 1999; Jazwinska et al., 1999) (Figures 5G and 5H). Repression of *brk* accounts for most of the effects of DPP in imaginal discs (Martin et al., 2004; Muller et al., 2003). Overexpression of either gene thus functionally mimics loss of function of DPP signaling.

Both DAD- and BRK-expressing *AyGal4:PR* clones exerted similar effects on BrdU labeling patterns in wing imaginal discs, although the effects of the *UAS-brk* transgene were reproducibly stronger (Figure 6). BrdU labeling within clones is reduced within 5 hr after induction, consistent with studies that have identified essential autonomous requirements for DPP signaling in wing-cell proliferation (Burke and Basler, 1996; Lecuit et al., 1996). Importantly, however, an increase in BrdU labeling is observed adjacent to medial clones. This nonautonomous stimulation of BrdU labeling can be detected as early as 5 hr after induction and was readily observable at 14 and 20 hr time points (Figure 6 and data not shown). The elevated BrdU labeling is greatest along the most medial edges of clones (Figure 6), consistent with the hypothesis that the degree of stimulation is dependent upon the degree of difference in positional values between neighboring cells. Lower-level expression of BRK resulted in weaker, but qualitatively similar, effects on BrdU labeling (Figure 6E). Although induction of BRK expression in conventional Flp-out clones has been associated with cell competition and apoptosis (Moreno et al., 2002), no apoptosis occurred within the first 26 hr after its induction in *AyGal4:PR* clones, presumably because large groups of cells are protected from cell competition. At 48 hr, a few apoptotic cells were detected along the edges of BRK-expressing clones (data not shown), but this is too late to account for the nonautonomous stimulation of proliferation observed.

## Discussion

### Juxtaposing Cells that Perceive Different Levels of DPP Signaling Stimulates Proliferation

A class of models for growth control have posited that growth is promoted by the juxtaposition of cells with different positional values. While the elegance of such models has been widely appreciated, until now, they have suffered from a lack of experimental support, as studies of morphogens that actually regulate growth in developing tissues have appeared to argue against them. However, by exercising spatial, temporal, and quantitative control over expression of components of the DPP pathway, we have obtained compelling evidence in support of the hypothesis that wing growth is influenced by a gradient of positional values estab-

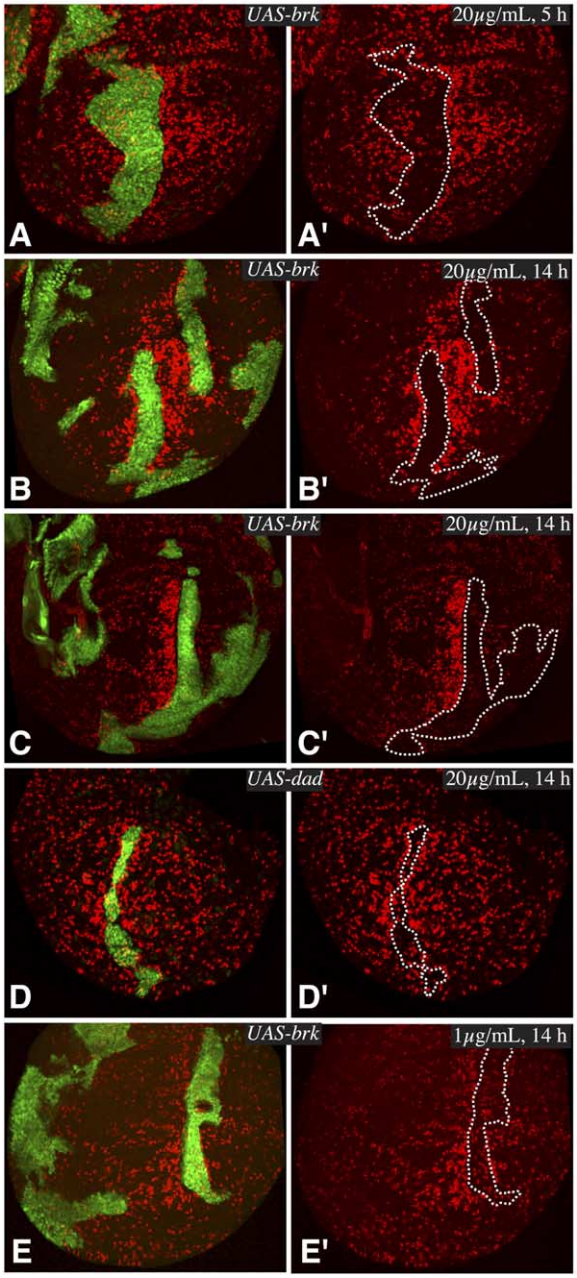


Figure 6. Clonal Induction of BRK or DAD Induces Nonautonomous Cell Proliferation

All panels show discs containing Gal4:PR-expressing clones from animals with *AyGal4:PR UAS-p35 UAS-GFP* and either *UAS-brk* or *UAS-dad* transgenes, marked by expression of GFP (green) and grown for the indicated number of hours on media containing RU486 at 20 μg/ml (A–D) or 1 μg/ml (E) and then labeled and stained for BrdU (red). (A)–(C) and (E) show BRK-expressing clones; (D) shows a DAD-expressing clone.

lished downstream of DPP. Juxtaposing cells with different levels of DPP pathway activity stimulates cell proliferation, as revealed by molecular markers of cell-cycle progression. This stimulation can be achieved by either elevating or lowering the level of pathway activity relative to that in neighboring cells, and the effect is proportional to the difference in pathway activity. Conversely, activating TKV uniformly inhibits cell proliferation in medial wing cells, where the endogenous gradient is normally steep. Together, these observations indicate that a difference in levels of DPP signaling between adjacent cells is both necessary and sufficient for the proliferation of medial wing cells and thereby implicate the slope of the DPP morphogen gradient as the driving force behind medial-wing-cell proliferation during normal development.

The prior failure to discern the importance of the DPP gradient in growth regulation can be accounted for by two aspects of the proliferative response. First, the transience of the nonautonomous response under experimental conditions precluded its observation using the protocols traditionally employed for examining $TKV^{Q\text{-}D}$-expressing clones, which allow clones to grow for two or more days. Even when we examined such clones after only 1 day (data not shown), their small size made their ability to stimulate proliferation nonautonomously less obvious than with the larger $TKV^{Q\text{-}D}$ clones generated by the *AyGal4:PR* method. Second, the overgrowth of lateral regions had obscured, until direct observations of proliferation were conducted (Figure 5) (Martin et al., 2004), the inhibition of medial-cell proliferation associated with uniform TKV activation.

## Modeling Growth Control by a Morphogen Gradient

We outline here a mechanism by which the TKV activity gradient could regulate proliferation (Figure 7A). Although we expect the actual mechanism to be more complex, the model proposed serves to illustrate some basic principles. The ability to compare TKV activity levels between adjacent cells likely requires the participation of a cell-surface molecule, which we will call X, regulated downstream of TKV. We assume that expression of X is positively regulated downstream of TKV, presumably via repression of *brk*. In the simplest case, a comparison between expression levels on adjacent cells could be made by homophilic binding. In this case, the number of bound molecules on the surfaces of adjacent cells would be equal and hence convey no information as to the relative levels between them. However, the fraction of molecules unbound would be proportional to the elevated levels of X in one cell as compared to its neighbor, and, thus, unbound X could stimulate proliferation (Figure 7A).

Our observations indicate that the stimulation of proliferation is bidirectional (i.e., it can occur on the high or the low side of differences in TKV activity; Figure 3 and Figure 6) and that it can spread over a few cells. Although this might suggest the participation of a diffusible molecule downstream of X, it could also occur if X can be asymmetrically localized within a cell, X activity influences X localization, and asymmetric X localization can be propagated from cell to cell. Exactly this sort of process occurs during the establishment of tissue polarity (reviewed in Eaton, 2003), and it has been suggested to involve a local feedback loop between adjacent cells amplifying an initial asymmetry (Amonlirdviman et al., 2005). It is intriguing in this regard that two of the most upstream regulators of tissue polarity, Fat and Dachsous, are transmembrane proteins that also exert substantial effects on imaginal-disc growth,

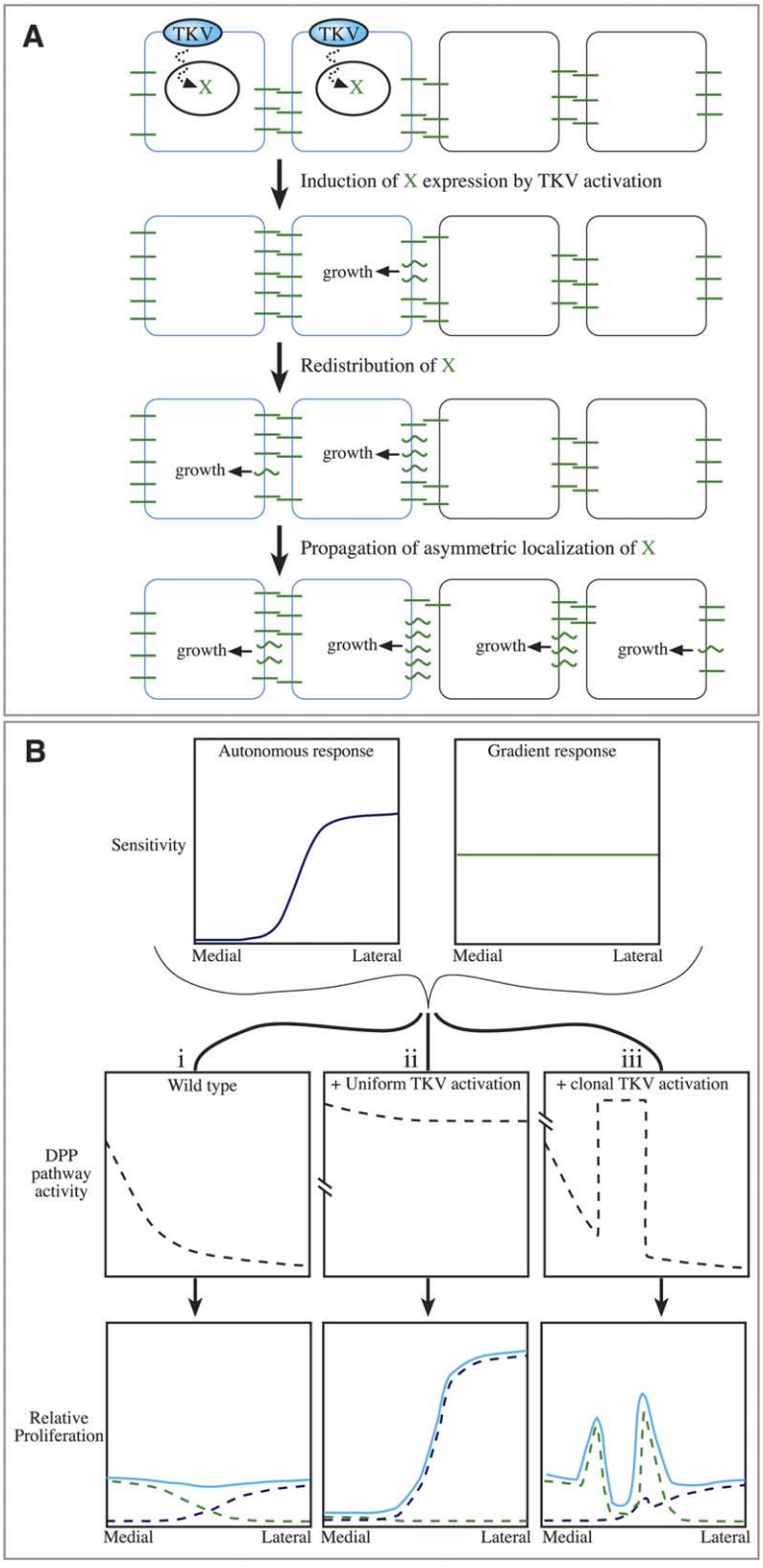


Figure 7. Modeling Growth Regulation by a Morphogen Gradient

(A) The schematic illustrates a mechanism by which the slope of the TKV activity gradient could regulate growth. We suggest that TKV could regulate the expression of a transmembrane protein, X (green bars). X participates in homophilic interactions. In cases where the amounts of X are unequal between neighboring cells, a significantly greater fraction of X will be unbound in the cell with more X. Unbound X (squiggly green bars) transmits a signal that promotes growth and also modulates the localization of X, such that X preferentially accumulates at cell interfaces where it is unbound and is removed from interfaces where it is bound. As in mechanisms that have been suggested for the propagation of tissue polarity, this redistribution of X could propagate from cell to cell, allowing some promotion of growth even between neighbors with similar levels of X, with the range depending on the efficiency of the propagation mechanism.

(B) The schematic illustrates the expected contributions of the proposed autonomous and gradient responses to TKV activity. The sensitivity (top) of cells to the autonomous-proliferation response varies across the medial-lateral aspect of the wing (blue line), while the gradient response occurs throughout (green line). (i) In combination with the wild-type TKV activity gradient (black dashed line), the gradient response pathway can promote proliferation (green dashed line) that is proportional to the slope of the activity gradient. The autonomous pathway can promote proliferation (blue dashed line) in lateral cells, but it is limited by the low levels of TKV activity here. When summed together (solid cyan line), the pathways effect roughly even proliferation across the disc. (ii) When $TKV^{Q\text{-}D}$ is expressed ubiquitously, the gradient is shallow even in medial regions (hatch marks indicate interrupted scale), so no proliferation occurs here, while the combination of high sensitivity and high pathway activation results in elevated proliferation in lateral regions. (iii) When $TKV^{Q\text{-}D}$ is expressed in clones, the juxtaposition in fates at the clone edge is even steeper than the endogenous gradient and so is able to stimulate elevated proliferation.

and it is conceivable that they act as critical mediators between morphogen gradients and tissue growth (Casal et al., 2002; Lawrence, 2004). We suggest that both activation and inhibition of the DPP pathway result in nonautonomous stimulation of proliferation because both result in a self-reinforcing, asymmetric distribution of X, allowing a proliferative signal to be generated in cells on either side of an expression boundary (Figure

7A). One attraction of this mechanism is that, as hypothesized for tissue polarity (Ma et al., 2003), a self-reinforcing asymmetry mechanism would allow for some buffering against local variations in the morphogen gradient and thus further contribute to the even distribution of growth.

In our experimental situations, we suggest that uniform activation of TKV in medial cells blocks proliferation by swamping out the endogenous gradient of X. $TKV^{Q-D}$ clones, by contrast, create a sharp juxtaposition in cell fates, leading to propagation of X asymmetry from the clone edges. Within these clones, the high, uniform activation of TKV would inhibit X activation and counteract the ability to establish an asymmetry of X, thereby decreasing proliferation relative to that induced outside of the clones—although we emphasize that proliferation within these clones (Figure 3) is greater than occurs under uniform TKV activation (Figure 5), suggesting that some X asymmetry does propagate into the clones. When X levels are decreased in clones, as by expression of BRK, X asymmetry can propagate well outside the clones, but, inside the clones, low levels of X limit both proliferation and the propagation of X asymmetry. This type of model thus provides an explanation for the seemingly paradoxical observation that proliferation is preferentially stimulated on the outside of both $TKV^{Q-D}$- and BRK-expressing clones.

Another intriguing feature of $TKV^{Q-D}$ clones is the transience of the response. This suggests that, like most signaling pathways, X signaling is subject to negative feedback that can dampen the response. This might function during normal development to limit tissue growth. The differences between cells are more extreme in our experiments than those that normally occur during disc development. Because of this, the negative feedback might be more robust than normal, resulting in a more transient effect. Our experimental paradigm also introduces an artificial stability to the differences in TKV activity between neighboring cells, whereas, in a normal developing disc, the DPP gradient and cell locations within it are dynamic. This could also influence the efficiency of the hypothesized negative feedback. The transience and short range of the nonautonomous proliferative response associated with $TKV^{Q-D}$ clones are likely factors in the apparent absence of extensive nonautonomous overgrowth associated with $TKV^{Q-D}$ clones in adult flies.

## Distinct Strategies for Growth Regulation across the DPP Morphogen Gradient

Our results indicate that there are two distinct mechanisms by which the DPP pathway regulates growth, one that depends on the gradient of DPP and another that depends on the level of DPP. Notably, these distinct mechanisms correlate with different aspects of the DPP gradient. That is, while juxtaposition of cells that perceive different levels of TKV activity can promote proliferation throughout the wing, during normal development, this effect is likely only significant in medial regions, as the TKV activity gradient is steep medially but shallow laterally (Tanimoto et al., 2000; Teleman and Cohen, 2000). Conversely, TKV activity also promotes proliferation cell autonomously, presumably via repression of *brinker*, but this response is restricted to lateral regions (Figure 5) (Martin et al., 2004), where endogenous levels of DPP are normally low and the gradient is shallow.

One complication with gradient models for growth control is that morphogen gradients tend to decay exponentially rather than linearly (Entchev et al., 2000; Teleman and Cohen, 2000). Importantly then, the existence of these two distinct mechanisms for growth regulation by DPP signaling suggests an explanation for how a relatively even distribution of cell proliferation could be achieved across a morphogen gradient. To illustrate this, we sketch the expected contributions of the gradient and autonomous-proliferation mechanisms across the medial-lateral aspect of a wing disc (Figure 7B). Applying the same approach to our experimental situations, one can visualize that the lack of proliferation in medial cells upon uniform TKV activation would be a consequence of the relative smoothing of the activity gradient and that overproliferation in lateral cells is expected to be driven entirely by the autonomous mechanism. Conversely, the overproliferation in medial cells associated with clonal activation of TKV is expected to result from the gradient mechanism. Moreover, given that the endogenous rate of medial-cell proliferation is predicted to reflect the response to the endogenous gradient, significantly elevated rates of proliferation in experimental situations are expected to require a significantly steeper than normal juxtaposition in cell fates.

## Experimental Procedures

### Construction of pAyGal4:PR

pAyGal4:PR was constructed by cloning a 2 kb NheI-BamHI fragment containing the GeneSwitch Gal4 cDNA from the pP(GS-GAL4) vector (Osterwalder et al., 2001) into NheI/BamHI-digested pWA-GAL4-Nhe (Ito et al., 1997), replacing the wild-type Gal4, to generate a plasmid we refer to as pWAGal4:PR-Nhe. We then cloned a 9.7 kb NheI fragment containing an *FRT/y+/FRT* cassette from plasmid pJ35 (Struhl and Basler, 1993) into the NheI site of pWA-GAL4:PR-Nhe, which placed the *FRT/y+/FRT* cassette between the *actin* promoter and the *Gal4:PR* coding sequence. The resulting plasmid, pAyGal4:PR, was injected into *Drosophila*, and insertions on the X (*AyGal4:PR[X]*) and third (*AyGal4:PR[3]*) chromosomes were isolated. Results shown were generated with *AyGal4:PR[3].*

### Clone Generation and Transgene Induction

For generation of Flp-out clones, flies of the genotypes *y w hs-Flp[122];UAS-tkv$^{Q253D}$/TM6b*, *y w hs-Flp[122];UAS-tkv$^{DEQ199D}$[6A3]*, *y w hs-Flp[122];UAS-p35[2-Y];UAS-tkv$^{Q253D}$/TM6b*, *y w hs-Flp[122];UAS-p35[2-Y];UAS-tkv$^{DEQ199D}$[6A3]*, *y w hs-Flp[122];UAS-cycD UAS-cdk4/L14*, *y w hs-Flp[122];UAS-p35[2-Y];UAS-brk[S7.1]*, *y w hs-Flp[122];UAS-dad;UAS-p35[3-W]*, *y w hs-Flp[122];UAS-p35[2-Y]*, *y w hs-Flp[122]*, and *y w hs-Flp[122];dpp-lacZ[10638]/CyO-GFP; UAS-tkv$^{Q253D}$/TM6b* were crossed to *UAS-GFP;AyGal4:PR[3]/TM6b* flies. Flp-out clones were then generated by heat shock for 7 min at 36°C. *PCNA-GFP;AyGal4:PR[3]* flies were crossed to *y w hs-Flp [122];UAS-p35[2-Y];UAS-tkv$^{Q253D}$/TM6b* (experimental) or *y w hs-Flp[122];UAS-p35[2-Y]* (control).

For ubiquitous transgene expression, flies in which the *FRT/y+/Terminator* cassette had been excised were selected from a *y w hs-Flp[122];AyGal4:PR[3]/TM6b* stock by the loss of the *y+* marker to isolate the *actin>Gal4:PR[3]* transgene insertion. *y w hs-Flp [122];UAS-GFP; actin>Gal4:PR[3]/TM6b* flies were then crossed to *y w hs-Flp[122];UAS-tkv$^{Q253D}$/TM6b*, *y w hs-Flp[122] omb-lacZ; UAS-tkv$^{Q253D}$/TM6b*, *y w hs-Flp[122] omb-lacZ*, *brk-lacZ;UAS-tkv$^{Q253D}$/TM6b*, *brk-lacZ*, or *y w hs-Flp[122];UAS-GFP* flies.

Gal4:PR was activated by transfer of larvae to instant food (Instant *Drosophila* Medium, Connecticut Valley Biological) containing RU486 (mifepristone, Sigma). Two grams of instant food was mixed with 7 ml RU486 in water, resulting in a final medium volume of approximately 8.5 ml. The RU486 solutions were 24 μg/ml for high-dose experiments and 1.2 μg/ml for low-dose experiments, resulting in final effective concentrations of 20 μg/ml and 1 μg/ml.

### Tissue Staining and BrdU Labeling

For BrdU labeling, larvae were dissected in Ringers solution and then incubated in M3 complete medium containing 0.1 mg/ml BrdU (BD Pharmingen) for 30 min at room temperature. After three rinses with cold PTW (PBS, 0.1% Tween 20), larvae were fixed for 20 min in 4% paraformaldehyde plus 0.1% Tween 20. Larvae were then washed four times for 20 min in PTW and then treated with 5 units DNase I (Promega) in 100 μl DNase buffer + PBS for 1.5 hr at 37°C. After three washes in PTW, larvae were incubated with anti-BrdU.

Blind scoring of BrdU, pH-H3, or PCNA-GFP staining was accomplished by having D.R. take confocal micrographs of all clones in a set of experimental and control stains, having a third party assign them random numbers, and then having K.D.I. score clones for effects on staining.

Primary antibodies used were mouse anti-BrdU (BD Pharmingen), rabbit anti-activated Drice (B. Hay), rabbit anti-phosophorylated MAD (T. Tabata and E. Laufer), rabbit anti-pH-H3 (Upstate), rabbit anti-Gal4 DBD (Santa Cruz), goat anti-β-Gal (Biogenesis), mouse anti-WG (4D4, DSHB), rat anti-Spalt (S. Cohen), and guinea pig anti-Coracle (R. Fehon). Secondary antibodies were from Jackson ImmunoResearch. DNA was stained by mounting discs in DAPI-containing media (Vector). β-galactosidase activity was detected by a standard X-gal staining protocol overnight at room temperature.

### Supplemental Data

Supplemental Data include one table and two figures and can be found with this article online at http://www.cell.com/cgi/content/full/123/3/449/DC1/.

### Acknowledgments

We thank K. Basler, S. Cohen, R. Duronio, B. Edgar, R. Fehon, B. Hay, Y. Hiromi, E. Laufer, R. Mann, T. Osterwalder, R. Padgett, C. Rushlow, G. Struhl, T. Tabata, M. O'Connor, I. Hariharan, the Developmental Studies Hybridoma Bank, and the Bloomington Stock Center for reagents; T. Correia and P. Woronoff for technical assistance; M. Crickmore for Figures 1B and 1C; K. Basler, M. Crickmore, L. Johnston, P. Lawrence, R. Padgett, C. Rauskolb, and G. Struhl for comments on the manuscript and helpful discussions; and the Howard Hughes Medical Institute for support.

Received: January 31, 2005
Revised: May 16, 2005
Accepted: August 22, 2005
Published: November 3, 2005

### References

Adachi-Yamada, T., and O'Connor, M.B. (2002). Morphogenetic apoptosis: a mechanism for correcting discontinuities in morphogen gradients. Dev. Biol. *251*, 74–90.

Adachi-Yamada, T., Fujimura-Kamada, K., Nishida, Y., and Matsumoto, K. (1999). Distortion of proximodistal information causes JNK-dependent apoptosis in *Drosophila* wing. Nature *400*, 166–169.

Amonlirdviman, K., Khare, N.A., Tree, D.R., Chen, W.S., Axelrod, J.D., and Tomlin, C.J. (2005). Mathematical modeling of planar cell polarity to understand domineering nonautonomy. Science *307*, 423–426.

Bohn, H. (1974). Extent and properties of the regeneration field in the larval legs of cockroaches (Leucophaea maderae) III. Origin of the tissues and determination of symmetry properties in the regenerates. J. Embryol. Exp. Morphol. *32*, 81–98.

Brand, A.H., and Perrimon, N. (1993). Targeted gene expression as a means of altering cell fates and generating dominant phenotypes. Development *118*, 401–415.

Burke, R., and Basler, K. (1996). Dpp receptors are autonomously required for cell proliferation in the entire developing *Drosophila* wing. Development *122*, 2261–2269.

Campbell, G., and Tomlinson, A. (1999). Transducing the Dpp morphogen gradient in the wing of *Drosophila*: regulation of Dpp targets by brinker. Cell *96*, 553–562.

Capdevila, J., and Guerrero, I. (1994). Targeted expression of the signaling molecule decapentaplegic induces pattern duplications and growth alterations in *Drosophila* wings. EMBO J. *13*, 4459–4468.

Casal, J., Struhl, G., and Lawrence, P. (2002). Developmental compartments and planar polarity in Drosophila. Curr. Biol. *12*, 1189–1198.

Datar, S.A., Jacobs, H.W., de la Cruz, A.F., Lehner, C.F., and Edgar, B.A. (2000). The *Drosophila* cyclin D-Cdk4 complex promotes cellular growth. EMBO J. *19*, 4543–4554.

Day, S.J., and Lawrence, P.A. (2000). Measuring dimensions: the regulation of size and shape. Development *127*, 2977–2987.

Eaton, S. (2003). Cell biology of planar polarity transmission in the Drosophila wing. Mech. Dev. *120*, 1257–1264.

Entchev, E.V., Schwabedissen, A., and Gonzalez-Gaitan, M. (2000). Gradient formation of the TGF-β homolog Dpp. Cell *103*, 981–991.

French, V., Bryant, P.J., and Bryant, S.V. (1976). Pattern regulation in epimorphic fields. Science *193*, 969–981.

Garcia-Bellido, A., and Merriam, J.R. (1971). Parameters of the wing imaginal disc development of Drosophila melanogaster. Dev. Biol. *24*, 61–87.

Garcia-Bellido, A.C., and Garcia-Bellido, A. (1998). Cell proliferation in the attainment of constant sizes and shapes: the Entelechia model. Int. J. Dev. Biol. *42*, 353–362.

Gelbart, W.M. (1989). The decapentaplegic gene: a TGF-beta homologue controlling pattern formation in Drosophila. Development *107*, 65–74.

Gibson, M.C., Lehman, D.A., and Schubiger, G. (2002). Lumenal transmission of decapentaplegic in Drosophila imaginal discs. Dev. Cell *3*, 451–460.

Haerry, T.E., Khalsa, O., O'Connor, M.B., and Wharton, K.A. (1998). Synergistic signaling by two BMP ligands through the SAX and TKV receptors controls wing growth and patterning in Drosophila. Development *125*, 3977–3987.

Huh, J.R., Guo, M., and Hay, B.A. (2004). Compensatory proliferation induced by cell death in the Drosophila wing disc requires activity of the apical cell death caspase Dronc in a nonapoptotic role. Curr. Biol. *14*, 1262–1266.

Irvine, K.D., and Rauskolb, C. (2001). Boundaries in development: formation and function. Annu. Rev. Cell Dev. Biol. *17*, 189–214.

Ito, K., Awano, W., Suzuki, K., Hiromi, Y., and Yamamoto, D. (1997). The Drosophila mushroom body is a quadruple structure of clonal units each of which contains a virtually identical set of neurones and glial cells. Development *124*, 761–771.

Jazwinska, A., Kirov, N., Wieschaus, E., Roth, S., and Rushlow, C. (1999). The Drosophila gene brinker reveals a novel mechanism of Dpp target gene regulation. Cell *96*, 563–573.

Lawrence, P.A. (1970). Polarity and patterns in the postembryonic development of insects. Adv. Insect Physiol. *7*, 197–266.

Lawrence, P.A. (2004). Last hideout of the unknown? Nature *429*, 247.

Lawrence, P.A., and Struhl, G. (1996). Morphogens, compartments, and pattern: lessons from *Drosophila*?. Cell *85*, 951–961.

Lecuit, T., and Cohen, S.M. (1998). Dpp receptor levels contribute to shaping the Dpp morphogen gradient in the Drosophila wing imaginal disc. Development *125*, 4901–4907.

Lecuit, T., Brook, W.J., Ng, M., Calleja, M., Sun, H., and Cohen, S.M. (1996). Two distinct mechanisms for long-range patterning by Decapentaplegic in the Drosophila wing. Nature *381*, 387–393.

Ma, D., Yang, C.H., McNeill, H., Simon, M.A., and Axelrod, J.D. (2003). Fidelity in planar cell polarity signalling. Nature *421*, 543–547.

Martin, F.A., Perez-Garijo, A., Moreno, E., and Morata, G. (2004). The brinker gradient controls wing growth in Drosophila. Development *131*, 4921–4930.

Martin-Castellanos, C., and Edgar, B.A. (2002). A characterization of the effects of Dpp signaling on cell growth and proliferation in the Drosophila wing. Development *129*, 1003–1013.

Milan, M., Campuzano, S., and Garcia-Bellido, A. (1996). Cell cycling and patterned cell proliferation in the wing primordium of Drosophila. Proc. Natl. Acad. Sci. USA *93*, 640–645.

Moreno, E., Basler, K., and Morata, G. (2002). Cells compete for decapentaplegic survival factor to prevent apoptosis in Drosophila wing development. Nature *416*, 755–759.

Muller, B., Hartmann, B., Pyrowolakis, G., Affolter, M., and Basler, K. (2003). Conversion of an extracellular Dpp/BMP morphogen gradient into an inverse transcriptional gradient. Cell *113*, 221–233.

Nellen, D., Burke, R., Struhl, G., and Basler, K. (1996). Direct and long-range action of a DPP morphogen gradient. Cell *85*, 357–368.

Osterwalder, T., Yoon, K.S., White, B.H., and Keshishian, H. (2001). A conditional tissue-specific transgene expression system using inducible GAL4. Proc. Natl. Acad. Sci. USA *98*, 12596–12601.

Padgett, R.W. (1999). Intracellular signaling: Fleshing out the TGFbeta pathway. Curr. Biol. *9*, R408–R411.

Perez-Garijo, A., Martin, F.A., and Morata, G. (2004). Caspase inhibition during apoptosis causes abnormal signalling and developmental aberrations in Drosophila. Development *131*, 5591–5598.

Resino, J., Salama-Cohen, P., and Garcia-Bellido, A. (2002). Determining the role of patterned cell proliferation in the shape and size of the Drosophila wing. Proc. Natl. Acad. Sci. USA *99*, 7502–7507.

Roman, G., Endo, K., Zong, L., and Davis, R.L. (2001). P[Switch], a system for spatial and temporal control of gene expression in Drosophila melanogaster. Proc. Natl. Acad. Sci. USA *98*, 12602–12607.

Ryoo, H.D., Gorenc, T., and Steller, H. (2004). Apoptotic cells can induce compensatory cell proliferation through the JNK and the Wingless signaling pathways. Dev. Cell *7*, 491–501.

Serrano, N., and O'Farrell, P.H. (1997). Limb morphogenesis: connections between patterning and growth. Curr. Biol. *7*, R186–R195.

Spencer, F.A., Hoffmann, F.M., and Gelbart, W.M. (1982). Decapentaplegic: a gene complex affecting morphogenesis in Drosophila melanogaster. Cell *28*, 451–461.

Struhl, G., and Basler, K. (1993). Organizing activity of wingless protein in Drosophila. Cell *72*, 527–540.

Tanimoto, H., Itoh, S., ten Dijke, P., and Tabata, T. (2000). Hedgehog creates a gradient of DPP activity in Drosophila wing imaginal discs. Mol. Cell *5*, 59–71.

Teleman, A.A., and Cohen, S.M. (2000). Dpp gradient formation in the Drosophila wing imaginal disc. Cell *103*, 971–980.

Thacker, S.A., Bonnette, P.C., and Duronio, R.J. (2003). The contribution of E2F-regulated transcription to Drosophila PCNA gene function. Curr. Biol. *13*, 53–58.

Tsuneizumi, K., Nakayama, T., Kamoshida, Y., Kornberg, T.B., Christian, J.L., and Tabata, T. (1997). Daughters against dpp modulates dpp organizing activity in Drosophila wing development. Nature *389*, 627–631.

Wolpert, L. (1969). Positional information and the spatial pattern of cellular differentiation. J. Theor. Biol. *25*, 1–47.

Zecca, M., Basler, K., and Struhl, G. (1995). Sequential organizing activities of engrailed, hedgehog, and decapentaplegic in the *Drosophila* wing. Development *121*, 2265–2278.